Noise- and inertia-induced inhomogeneity in the distribution of small particles in fluid flows

Julyan H. E. Cartwright[a)]
Laboratorio de Estudios Cristalográficos, CSIC, E-18071 Granada, Spain

Marcelo O. Magnasco[b)]
Mathematical Physics Laboratory, Rockefeller University, P.O. Box 212, 1230 York Avenue, New York, New York 10021

Oreste Piro[c)]
Institut Mediterrani d'Estudis Avançats, CSIC–UIB, E-07071 Palma de Mallorca, Spain

(Received 2 November 2001; accepted 25 March 2002; published 20 May 2002)

The dynamics of small spherical neutrally buoyant particulate impurities immersed in a two-dimensional fluid flow are known to lead to particle accumulation in the regions of the flow in which vorticity dominates over strain, provided that the Stokes number of the particles is sufficiently small. If the flow is viewed as a Hamiltonian dynamical system, it can be seen that the accumulations occur in the nonchaotic parts of the phase space: the Kolmogorov–Arnold–Moser tori. This has suggested a generalization of these dynamics to Hamiltonian maps, dubbed a bailout embedding. In this paper we use a bailout embedding of the standard map to mimic the dynamics of neutrally buoyant impurities subject not only to drag but also to fluctuating forces modeled as white noise. We find that the generation of inhomogeneities associated with the separation of particle from fluid trajectories is enhanced by the presence of noise, so that they appear in much broader ranges of the Stokes number than those allowing spontaneous separation. © *2002 American Institute of Physics.* [DOI: 10.1063/1.1480441]

Impurities suspended in a fluid flow are frequently observed to be distributed inhomogeneously. Even in very chaotic flows, particulate impurities arrange themselves in extraordinarily structured distributions, in apparent contradiction to the high mixing efficiency expected from the characteristics of the basic flow. To give just one example, in the particular instance of geophysical fluids, the filamentary structure, or patchiness, often displayed by plankton populations in the oceans is a puzzling problem currently under intense investigation.[1–3] Several mechanisms to produce this type of inhomogeneity have been studied, and include dynamical aspects of the flow as well as the reactive properties of the considered impurities. The basic idea in many of these mechanisms is that the particle loss due either to the flow—in open flows—or to the chemical or population dynamics of the particles—in closed flows—is minimized on some manifolds associated with the hyperbolic character of the flow.[4–6] In this paper we explore an alternative purely dynamical mechanism for inhomogeneity with nonreactive particles in bounded flows. We show that particle inertial effects combined with fluctuating forces are capable of producing inhomogeneity even in cases in which the impurity and fluid densities match exactly.

[a)]Electronic mail: julyan@lec.ugr.es
[b)]Electronic mail: marcelo@sur.rockefeller.edu
[c)]Electronic mail: piro@imedea.uib.es

I. INTRODUCTION

When impurities have a different density to the fluid, it is intuitively clear that they will be expelled from rapidly rotating regions of the flow—for heavy particles—or attracted to the centers of these regions—for light particles—because of centrifugal effects.[7] However, it was recently demonstrated that neutrally buoyant particles also tend to settle in the rotation (vorticity)-dominated regions of a flow, but by a more subtle mechanism involving the separation between the fluid and particle trajectories that can occur in the opposite regions, i.e., in the areas of the flow dominated by strain.[8] However, this mechanism is only relevant when the flow gradients are of the order of the particle drag coefficient, a condition that may not be fulfilled in some physically interesting situations. We show here by means of a minimal model that this condition may be relaxed if a small amount of noise is added to the forces acting on the impurity.

Our approach is qualitative, in the sense that instead of considering a specific flow and the precise particle dynamics induced by it, we describe the system with an iterative map whose evolution contains the basic features of both the fluid flow and the particle dynamics: flow volume preservation, together with particle separation in the hyperbolic regions. The reason for moving to a discrete system is that in the map the phenomena that we describe may be understood more intuitively, while translating the results back to the flow case is immediate. The strategy of attempting to understand fluid-dynamical phenomena by using iterated maps amenable to the powerful artillery of dynamical-systems theory has proved successful on several different occasions. For ex-

ample, the structures of the chaotic advection induced by time-periodic three-dimensional incompressible flows were predicted by studying the qualitatively equivalent dynamics of three-dimensional volume-preserving maps.[9,10] Later, these structures were confirmed in realistic flows.[11–13] Other examples are the treatment of the propagation of combustion fronts in laminar flows by a qualitative map approach,[14] and the description of the formation of plankton population structures due to inhomogeneities of the nutrient sources.[15] Remarkably, in the instance we discuss in this paper, the procedure is also useful from the point of view of dynamical-systems theory, as it has suggested a new technique—bailout embedding—for the control of Hamiltonian chaos.[16]

The plan of the paper is as follows. First, we briefly review the classical model for the forces acting on a small spherical particle moving relative to the fluid in which it is immersed, and, concentrating on the case of a neutrally buoyant impurity, we trace the construction of a minimal model that makes evident the separation of particle and fluid trajectories in the regions in which the flow presents strong strain (Sec. II). On the basis of this model, we make a generalization that allows us to build a discrete mapping that represents the Lagrangian evolution of the fluid parcels as well as the dynamics of the particle (Sec. III). While this map displays particle–fluid separation when the bailout parameter γ, a function of the Stokes number, is relatively small, we show in Sec. IV that a small amount of noise, added to the dynamics of the particle to separate it continually from the flow, enhances the impact of the hyperbolic regions far beyond the values of γ required for separation in the deterministic case. Section V extends and formalizes these ideas with analytical arguments. Our conclusions are to be found in Sec. VI.

II. MAXEY–RILEY EQUATIONS AND MINIMAL MODEL

The equation of motion for a small, spherical particle in an incompressible fluid we term the Maxey–Riley equation,[8,17,18] which may be written as

$$\rho_p \frac{d\mathbf{v}}{dt} = \rho_f \frac{D\mathbf{u}}{Dt} + (\rho_p - \rho_f)\mathbf{g} - \frac{9\nu\rho_f}{2a^2}\left(\mathbf{v}-\mathbf{u}-\frac{a^2}{6}\nabla^2\mathbf{u}\right) - \frac{\rho_f}{2}\left(\frac{d\mathbf{v}}{dt} - \frac{D}{Dt}\left[\mathbf{u}+\frac{a^2}{10}\nabla^2\mathbf{u}\right]\right) - \frac{9\rho_f}{2a}\sqrt{\frac{\nu}{\pi}}\int_0^t \frac{1}{\sqrt{t-\zeta}}\frac{d}{d\zeta}\left(\mathbf{v}-\mathbf{u}-\frac{a^2}{6}\nabla^2\mathbf{u}\right)d\zeta, \tag{1}$$

where the derivative $D\mathbf{u}/Dt$ is along the path of a fluid element

$$\frac{D\mathbf{u}}{Dt} = \frac{\partial\mathbf{u}}{\partial t} + (\mathbf{u}\cdot\nabla)\mathbf{u}, \tag{2}$$

whereas the derivative $d\mathbf{u}/dt$ is taken along the trajectory of the particle

$$\frac{d\mathbf{u}}{dt} = \frac{\partial\mathbf{u}}{\partial t} + (\mathbf{v}\cdot\nabla)\mathbf{u}. \tag{3}$$

Here $\mathbf{v}$ represents the velocity of the particle, $\mathbf{u}$ that of the fluid, ρ_p the density of the particle, ρ_f the density of the fluid it displaces, ν the kinematic viscosity of the fluid, a, the radius of the particle, and $\mathbf{g}$, gravity. The terms on the right-hand side of Eq. (1) represent, respectively, the force exerted by the undisturbed flow on the particle, buoyancy, Stokes drag, the added mass due to the boundary layer of fluid moving with the particle,[19,20] and the Basset–Boussinesq force[21,22] that depends on the history of the relative accelerations of particle and fluid. The terms in $a^2\nabla^2\mathbf{u}$ are the Faxén[23] corrections. The Maxey–Riley equation is derived under the assumptions that the particle radius and its Reynolds number are small, as are the velocity gradients around the particle.

First let us consider a minimal model for a neutrally buoyant particle. For this we set $\rho_p = \rho_f$ in Eq. (1). We consider the Faxén corrections and the Basset–Boussinesq term to be negligible. We now rescale space, time, and velocity by scale factors L, $T = L/U$, and U, to arrive at

$$\frac{d\mathbf{v}}{dt} = \frac{D\mathbf{u}}{Dt} - \mathrm{St}^{-1}(\mathbf{v}-\mathbf{u}) - \frac{1}{2}\left(\frac{d\mathbf{v}}{dt} - \frac{D\mathbf{u}}{Dt}\right), \tag{4}$$

where St is the particle Stokes number $\mathrm{St} = 2a^2U/(9\nu L) = 2/9(a/L)^2\,\mathrm{Re}_f$, Re_f being the fluid Reynolds number. The assumptions involved in deriving Eq. (1) require that $\mathrm{St} \ll 1$ in Eq. (4).

If we substitute the expressions for the derivatives in Eqs. (2) and (3) into Eq. (4), we obtain

$$\frac{d}{dt}(\mathbf{v}-\mathbf{u}) = -((\mathbf{v}-\mathbf{u})\cdot\nabla)\mathbf{u} - \gamma(\mathbf{v}-\mathbf{u}), \tag{5}$$

where we have written $\gamma = 2/3\mathrm{St}^{-1}$. We may then write $\mathbf{A} = \mathbf{v}-\mathbf{u}$, whence

$$\frac{d\mathbf{A}}{dt} = -(J+\gamma I)\cdot\mathbf{A}, \tag{6}$$

where J is the velocity gradient matrix—we now concentrate on two-dimensional flows $\mathbf{u} = (u_x, u_y)$—

$$J = \begin{pmatrix} \partial_x u_x & \partial_y u_x \\ \partial_x u_y & \partial_y u_y \end{pmatrix}. \tag{7}$$

If we diagonalize this matrix, and heuristically assume that the dependence on time of the diagonalizing transformation is unimportant, we obtain

$$\frac{d\mathbf{A}_D}{dt} = \begin{pmatrix} \lambda-\gamma & 0 \\ 0 & -\lambda-\gamma \end{pmatrix}\cdot\mathbf{A}_D, \tag{8}$$

so if $\mathrm{Re}(\lambda) > \gamma$, $\mathbf{A}_D$ may grow exponentially. Now λ satisfies $\det(J-\lambda I) = 0$, so $\lambda^2 - \mathrm{tr}\,J + \det J = 0$. Since the flow is incompressible, $\partial_x u_x + \partial_y u_y = \mathrm{tr}\,J = 0$, thence $-\lambda^2 = \det J$. Given squared vorticity $\omega^2 = (\partial_x u_y - \partial_y u_x)^2$, and squared strain $s^2 = s_1^2 + s_2^2$, where the normal component is $s_1 = \partial_x u_x - \partial_y u_y$ and the shear component is $s_2 = \partial_y u_x + \partial_x u_y$, we may write

$$Q = \lambda^2 = -\det J = (s^2 - \omega^2)/4, \tag{9}$$

where Q is the Okubo–Weiss parameter.[24,25] If $Q>0$, $\lambda^2>0$, and λ is real, deformation dominates, as around hyperbolic points, whereas if $Q<0$, $\lambda^2<0$, and λ is complex, rotation dominates, as near elliptic points.

Equation (6), together with $d\mathbf{x}/dt=\mathbf{A}+\mathbf{u}$, define a dissipative dynamical system

$$d\boldsymbol{\xi}/dt=\mathbf{F}(\boldsymbol{\xi},t) \tag{10}$$

with constant divergence $\nabla\cdot\mathbf{F}=-2\gamma$ in the four dimensional phase space $\boldsymbol{\xi}=(x,y,A_x,A_y)$, so that while small values of St—large values of γ—allow for large values of the divergence, large values of St—small values of γ—force the divergence to be small. The Stokes number is the relaxation time of the particle back onto the fluid trajectories compared to the time scale of the flow—with larger St (smaller γ), the particle has more independence from the fluid flow. From Eq. (8), about areas of the flow near hyperbolic stagnation points with $Q>\gamma^2$, particle and flow trajectories separate exponentially. The result is that the particle can overcome Stokes drag and abandon the fluid trajectories in the neighborhood of the saddle points, to finally end up in a regular region of the flow. This effect implies that particles tend to stay away from the regions of strongest strain.

In earlier work[8] it was shown that when the flow is chaotic—for example for two-dimensional time-periodic incompressible flows—it is a consequence of this phenomenon that particles asymptotically settle on invariant tori, and, in general, explore the ordered regions of the base flow. In the following, we investigate further this behavior in a qualitative but more general framework based on iterative map modeling of the dynamics.

III. DISCRETE DYNAMICS DESCRIPTION

An examination of the dynamical system defining our minimal model for the behavior of neutrally buoyant particles shows that it is composed of some dynamics within some other larger set of dynamics. Equation (4) can be seen as an equation for a variable $\mathbf{A}$ that defines another equation of motion, $\mathbf{v}=\mathbf{u}$, for a fluid element, when $\mathbf{A}$ is zero. The inner dynamics is that representing the Lagrangian trajectories of the flow, and in two dimensions it is a Hamiltonian system. We may say that this Hamiltonian system—the fluid flow—is embedded in a larger dynamical system—the fluid–particle system—this time dissipative, whose trajectories may or may not converge to zero. If they do, the system ends up on the same trajectories as those of the smaller embedded system, but in general this need not be the case. The concept of some dynamics embedded within some other dynamics may be exploited within the framework of dynamical-systems theory to design techniques to reject unwanted trajectories of the original dynamics by making them unstable in the embedding, paralleling what the particles do in the fluid-dynamical case. We have dubbed this idea, which has obvious applications to control and targeting, a bailout embedding of a dynamical system.[16]

Trading generality for clarity, in this section we present an example of a bailout embedding for discrete-time dynamical sytems that closely represents all the qualitative aspects of the above-described impurity dynamics. Given a map $\mathbf{x}_{n+1}=\mathbf{T}(\mathbf{x}_n)$—$\mathbf{x}$ being a point in a space of arbitrary dimension—a bailout embedding is the second-order recurrence

$$\mathbf{x}_{n+2}-\mathbf{T}(\mathbf{x}_{n+1})=K(\mathbf{x}_n)(\mathbf{x}_{n+1}-\mathbf{T}(\mathbf{x}_n)), \tag{11}$$

where $K(\mathbf{x})$ is chosen such that $|K(\mathbf{x})|>1$ over the unwanted set of orbits, so that they become unstable in the embedding. In this discrete system, almost any expression written for the ordinary differential equation, Eq. (6), translates to something close to an exponential; in particular, stability eigenvalues have to be negative in the ordinary-differential-equation case to represent stability, while they have to be smaller than one in absolute value in the map case. In order to simulate the dynamics of particles, the operator $-(J+\gamma I)$ in the continuous system should translate into the particular choice

$$K(\mathbf{x})=e^{-\gamma}\nabla\mathbf{T} \tag{12}$$

in the map setting.

To represent qualitatively a chaotic two-dimensional incompressible base flow we choose a classical testbed of Hamiltonian systems, the area preserving standard map introduced by Chirikov and Taylor:

$$\mathbf{T}:(x_n,y_n)\rightarrow(x_{n+1},y_{n+1}), \tag{13}$$

where

$$\begin{aligned} x_{n+1}&=x_n+\frac{k}{2\pi}\sin(2\pi y_n),\\ y_{n+1}&=y_n+x_{n+1}, \end{aligned} \tag{14}$$

and k is the parameter controlling integrability. Recall that, in general, the dynamics defined by this map present a mixture of quasiperiodic motions occurring on the Kolmogorov–Arnold–Moser (KAM) tori, and chaotic ones, depending on the initial conditions. As the value of k is increased, the region dominated by chaotic trajectories pervades more and more of the phase space, except for increasingly small islands of KAM quasiperiodicity. Our qualitative description of the impurity dynamics, the bailout embedding of the standard map, is given by the coupled second-order iterative system defined by Eqs. (11)–(14).

Due to the area-preserving nature of the standard map, the two eigenvalues of the derivative matrix must multiply to one. If they are complex, this means that both have an absolute value of one, while if they are real, generically one of them will be larger than one and the other smaller. We can then separate the phase space into elliptic and hyperbolic regions corresponding to each of these two cases. If a trajectory of the original map lies entirely in the elliptic regions, the overall factor $\exp(-\gamma)$ damps any small perturbation away from it in the embedded system. But for chaotic trajectories that inevitably visit some hyperbolic regions, there exists a value of γ such that, for γ smaller than this, perturbations away from a standard-map trajectory are amplified instead of dying out in the embedding. As a consequence, these trajectories are expelled from the chaotic regions finally to settle in the elliptic KAM islands.

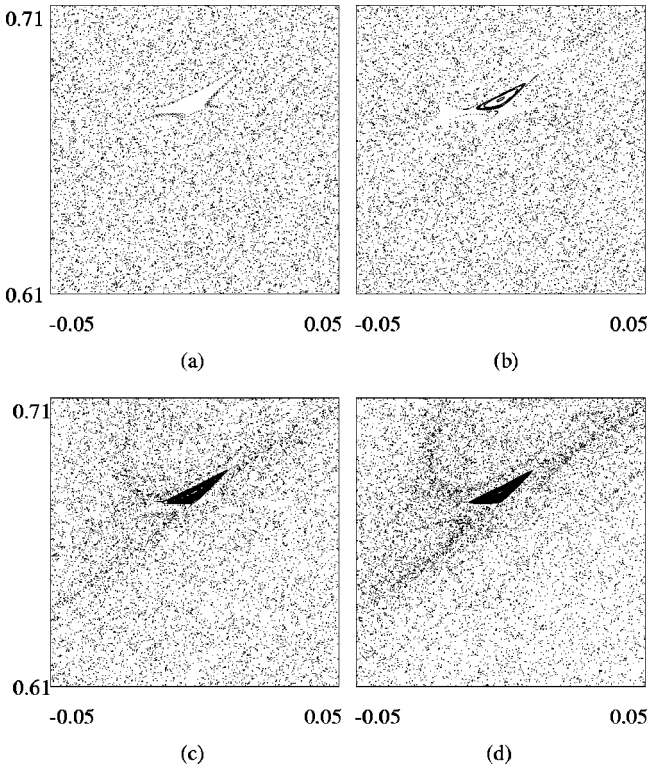

FIG. 1. The standard map for $k=7$ has a chaotic sea covering almost the entire torus, except for a tiny period-two KAM island near position 0,2/3. 1000 random initial conditions were chosen and iterated for 20000 steps, then the next 1000 iterations are shown. (a) Original map, (b) $\gamma=1.4$, (c) $\gamma=1.3$, (d) $\gamma=1.2$.

To illustrate this, Fig. 1 shows the phenomenon in a situation in which the nonlinearity parameter has been set to the value $k=7$. This corresponds to a very chaotic regime of the standard map, characterized by the existence of minute KAM islands within a sea of chaos that covers almost all the available phase space. Figure 1(a) is a close-up image—to make it easily visible—of the largest of these islands, and the dots there represent the successive positions of a set of 1000 fluid parcels spread initially at random over the unit cell, evolving according to the standard map. Since none of these parcels were initially located inside the island, this is seen as a white region never visited by the parcels. In contrast, in Figs. 1(b)–1(d), the dots are the successive positions, after a number of equilibration iterations, of particles initially placed as the parcels were in Fig. 1(a), but allowing a very small initial discrepancy $\boldsymbol{\delta}_0=\mathbf{x}_1-\mathbf{T}(\mathbf{x}_0)$ between the two dynamics. Now, although having started initially outside the island, some of the particles settle inside, in a process that becomes increasingly marked as the bailout parameter γ decreases.

IV. NOISY DYNAMICS

By virtue of volume preservation, the invariant measure of the fluid-parcel dynamics is either uniform, if the system is ergodic, or else disintegrates into a foliation of KAM tori and ergodic regions. In any case, the addition of a small amount of white noise, which may be considered to represent the effects of small scale turbulence, thermal fluctuations, etc., renders the system ergodic with only a uniform invariant measure. Thus, the distribution of fluid parcels is expected to be uniform with or without the presence of noise. The situation is, however, very different if the noise is applied to the dynamics of the particles, or, correspondingly, to the bailout embedding.

Consider the following stochastic discrete-time dynamics

$$\mathbf{x}_{n+2}-\mathbf{T}(\mathbf{x}_{n+1})=e^{-\gamma}\boldsymbol{\nabla}\mathbf{T}|_{\mathbf{x}_n}(\mathbf{x}_{n+1}-\mathbf{T}(\mathbf{x}_n))+\boldsymbol{\xi}_n, \qquad (15)$$

in which, as in Sec. III, $\mathbf{x}$ represents the particle coordinates and $\mathbf{T}(\mathbf{x})$ the fluid parcel evolution. New here is the noise term $\boldsymbol{\xi}_n$, with statistics

$$\langle\boldsymbol{\xi}_n\rangle=0, \quad \langle\boldsymbol{\xi}_n\boldsymbol{\xi}_m\rangle=\varepsilon(1-e^{-2\gamma})\delta_{mn}I. \qquad (16)$$

This term forces the particle away from the fluid trajectory at every step of the dynamics. However, the actual magnitude of the fluctuations induced in $\mathbf{x}$ will be modulated by the properties of $\boldsymbol{\nabla}\mathbf{T}$—the flow gradients—along the particle trajectory. For practical reasons we shall use the convention of varying the noise intensity in correspondence with γ in order to obtain comparable fluctuations at different values of this parameter.

We consider the standard map as modeling the basic flow, and its noisy bailout embedding to represent a particulate impurity subject to both fluid drag and noise forces. We are interested in the asymptotic behavior of an ensemble of such particles which, by the ergodicity of the fluctuations, should be well represented by the histogram of visits that a single particle pays over time to each bin of the space—the full phase space for the basic flow, but a projection of the full phase space for the particles.

Figure 2 displays a sequence of these histograms in a scaled color code for the same nonlinearity parameter, $k=7$, as in Fig. 1, corresponding to the extremely chaotic regime of the standard map considered in Sec. III. The sequence of images corresponds to decreasing bailout parameter γ. The images make evident the fine filamentary structure developed by the asymptotically invariant distributions due to the combined effects of noise and the ability of particles to separate from the basic flow. Remarkably, however, these structures appear even when the γ values are outside the range required to produce a spontaneous detachment of the particle trajectories without noise.

The filamentation here arises from the existence of avenues in the phase space that lead to the small KAM islands on which the particles prefer to stay. A more detailed analysis shows that on these avenues the average value of the squared separation between particle and fluid trajectories is relatively small. Roughly parallel to these avenues, on the other hand, there are strips of the phase space that the particles avoid. There, the separation between particle and fluid trajectories is on average much larger. Filamentation is thus due to the tendency of the particles to avoid neighboring regions.

The same mechanism may also lead to patchiness, not necessarily filamentary. For flows with weaker chaos, for example, for which relatively large KAM islands coexist with comparably sized regions of chaos, a situation such as that at

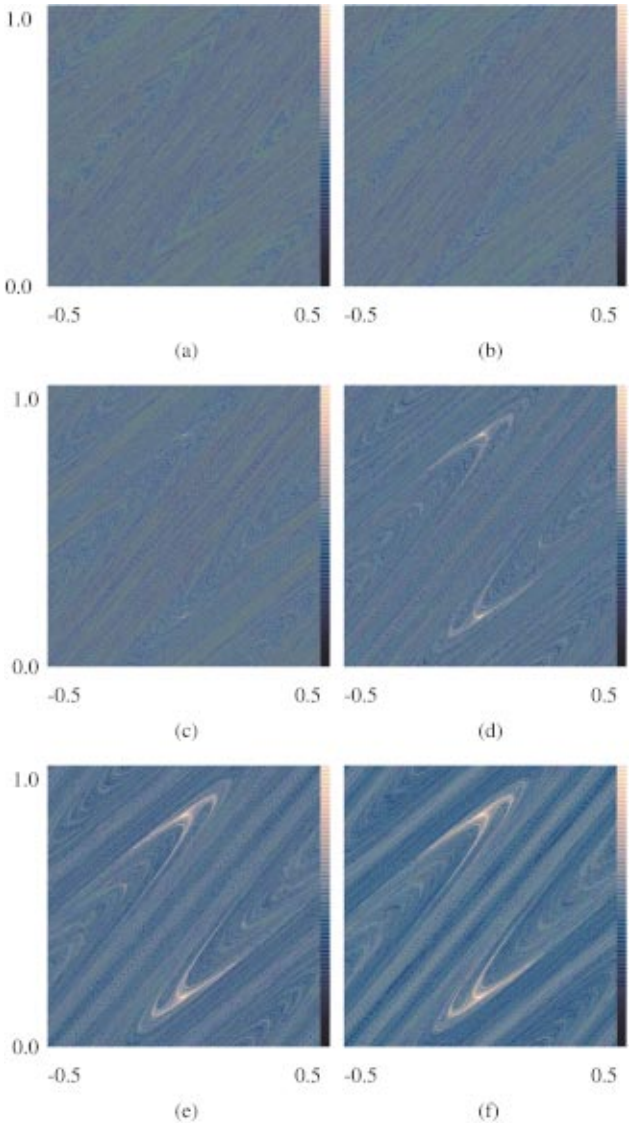

FIG. 2. (Color) Histograms with intensity encoding as the square root of invariant probability. Parameters are standard-map nonlinearity parameter $k=7$, noise parameter $\varepsilon=10^{-8}$, and bailout parameter (a) $\gamma=1.6$, (b) 1.55, (c) 1.5, (d) 1.4, (e) 1.3, and (f) 1.2. The striped color scale runs from pink at high densities to blue at low densities.

$k=1.5$, shown in Fig. 3, is typical. In the histograms, there are relatively small avoided regions that separate large patches of greater concentrations of particles around the nonchaotic islands. This picture is also testimonial to a property that distinguishes the present mechanism for producing inhomogeneity from others mentioned earlier.[4,5] While in those cases the particles group around the unstable manifolds of the homoclinic intersections of the basic flows, here the impurity dynamics instead tend to avoid the invariant manifolds. This is because following these manifolds would mean eventually hitting regions in which the velocity gradient eigenvalues are closer to one, which locally amplifies the effect of fluctuations on the dynamics of the particles.

V. DETACHMENT AND AVOIDANCE

We have seen earlier that inhomogeneities in the distribution of particles may arise at values of the Stokes number

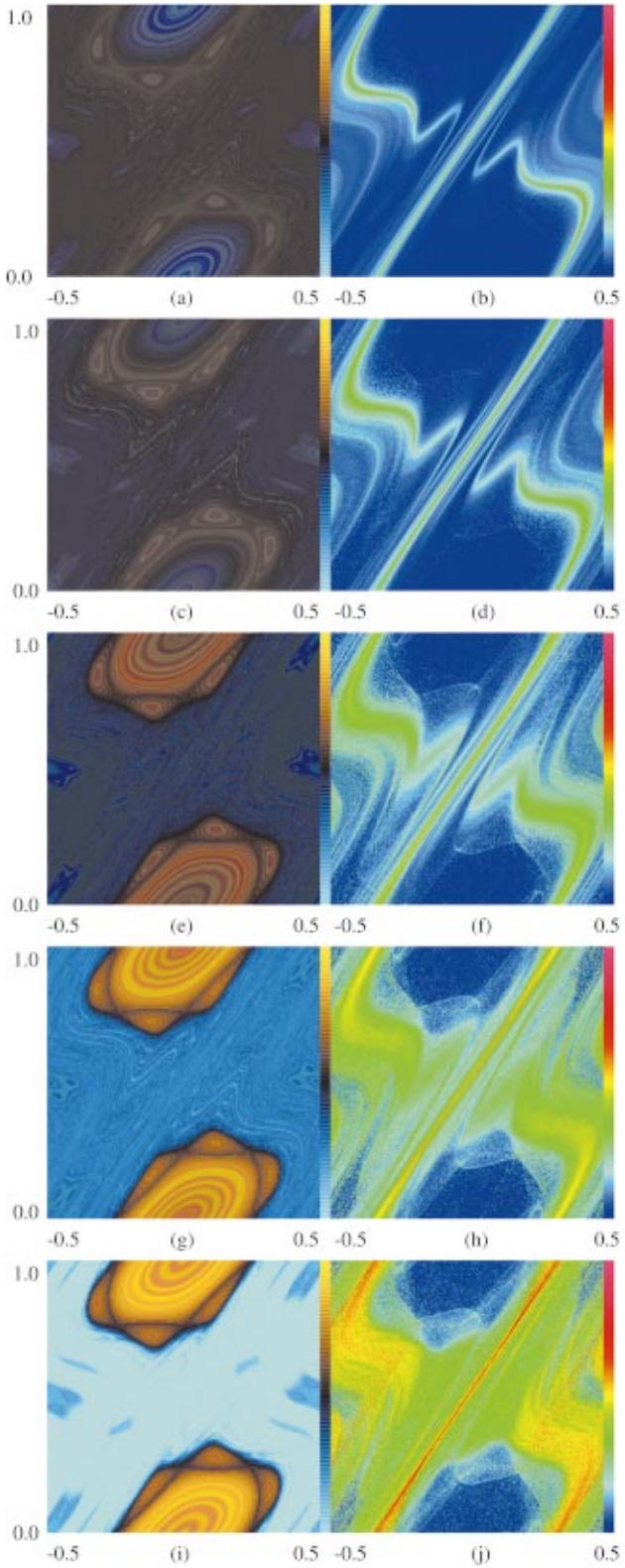

FIG. 3. (Color) Histograms (left-hand side) and temperature plots (right-hand side) for standard map nonlinearity parameter $k=1.5$, noise parameter $\varepsilon=10^{-8}$, and bailout parameter (a), (b), $\gamma=0.7$; (c), (d), $\gamma=0.65$; (e), (f), $\gamma=0.6$; (g), (h), $\gamma=0.55$; and (i), (j), $\gamma=0.5$. The striped histogram color scale runs from yellow at high densities to cyan at low densities, while the temperature color scale runs from red (high) to blue (low).

(or, equivalently, of the bailout parameter) beyond the range for which this phenomenon occurs in deterministic systems when a relatively small amount of noise is added to the particle dynamics, and hence, more generally, to the bailout dy-

namics. We show in the following that there are two stages to the modulation of the invariant density in the small-noise limit as the bailout parameter is decreased. At first the bailout is everywhere stable, as the bailout parameter is not small enough to occasion that the particle trajectories detach from the fluid ones, but fluctutations around this stable embedding may be restored toward the stable manifold at different rates, and thus acquire different expectation values. These fluctuations leave a mark on the invariant density through a mechanism similar to spatially modulated temperature,[26,27] namely, the dynamics prefer to escape the hot regions. This is balanced in a nontrivial fashion by mixing in the dynamics to create interesting scars in the invariant density. As the bailout parameter is lowered, the noise prefactor can diverge, the embedding loses stability at some points, and detachment ensues.

In order to analyze this critical transition, we proceed with the map approximation with the conviction that generalizing this analysis to the continuous-time limit is straightforward. We can separate the two-step recurrence, Eq. (15), into two one-step recurrences,

$$\mathbf{x}_{n+1}=\mathbf{T}(\mathbf{x}_n)+\boldsymbol{\delta}_n\,, \tag{17}$$

$$\boldsymbol{\delta}_{n+1}=e^{-\gamma}\boldsymbol{\nabla}\mathbf{T}|_{\mathbf{x}_n}\boldsymbol{\delta}_n+\boldsymbol{\xi}_n\,. \tag{18}$$

The second equation is affine, being linear in the $\boldsymbol{\delta}$ plus a homogeneously added noise process, so it could be solved analytically for $\boldsymbol{\delta}$ if we knew what the $\mathbf{x}$ were in the past. Under the assumption that the $\boldsymbol{\delta}$ are infinitesimally small, we get the classical orbits $\mathbf{x}_{n+1}=\mathbf{T}(\mathbf{x}_n)$, and we can write down explicitly the solution for the $\boldsymbol{\delta}$,

$$\begin{aligned}\boldsymbol{\delta}_{n+1}=\boldsymbol{\xi}_n+e^{-\gamma}\boldsymbol{\nabla}\mathbf{T}|_{\mathbf{x}_n}\times(\boldsymbol{\xi}_{n-1}+e^{-\gamma}\boldsymbol{\nabla}\mathbf{T}|_{\mathbf{x}_{n-1}}\\ \times(\boldsymbol{\xi}_{n-2}+e^{-\gamma}\boldsymbol{\nabla}\mathbf{T}|_{\mathbf{x}_{n-2}}(\boldsymbol{\xi}_{n-3}+\cdots)))),\end{aligned} \tag{19}$$

or, after unwrapping,

$$\begin{aligned}\boldsymbol{\delta}_{n+1}=\boldsymbol{\xi}_n+e^{-\gamma}\boldsymbol{\nabla}\mathbf{T}|_{\mathbf{x}_n}\boldsymbol{\xi}_{n-1}+e^{-2\gamma}\boldsymbol{\nabla}\mathbf{T}|_{\mathbf{x}_n}\boldsymbol{\nabla}\mathbf{T}|_{\mathbf{x}_{n-1}}\boldsymbol{\xi}_{n-2}\\ +e^{-3\gamma}\boldsymbol{\nabla}\mathbf{T}|_{\mathbf{x}_n}\boldsymbol{\nabla}\mathbf{T}|_{\mathbf{x}_{n-1}}\boldsymbol{\nabla}\mathbf{T}|_{\mathbf{x}_{n-2}}\boldsymbol{\xi}_{n-3}+\cdots,\end{aligned} \tag{20}$$

which may be written more compactly as

$$\boldsymbol{\delta}_{n+1}=\sum_{j=0}^{n}\left(\boldsymbol{\xi}_{n-j}e^{-j\gamma}\prod_{k=0}^{j}\boldsymbol{\nabla}\mathbf{T}|_{\mathbf{x}_{n-k}}\right). \tag{21}$$

Then, given that the $\boldsymbol{\xi}$ are uncorrelated, the expectation value of $\boldsymbol{\delta}^2$ is given as the sum of the squares of the terms, or

$$\frac{\langle\boldsymbol{\delta}^2\rangle}{\langle\boldsymbol{\xi}^2\rangle}=\sum_{j=0}^{\infty}\left(e^{-j\gamma}\prod_{k=0}^{j}\boldsymbol{\nabla}\mathbf{T}|_{\mathbf{x}_{n-k}}\right)^2, \tag{22}$$

where the $\langle\cdot\rangle$ are averages over the $\boldsymbol{\xi}$ process. Clearly, as $\gamma\to\infty$, this expression tends to 1.

In the regime in which $\gamma\gg 0$ and $\langle\boldsymbol{\xi}^2\rangle\ll 1$, the $\langle\boldsymbol{\delta}_{n+1}^2\rangle\approx\langle\boldsymbol{\xi}^2\rangle\ll 1$ and hence the trajectories collapse upon the classical orbits: $\mathbf{x}_{n+1}=\mathbf{T}(\mathbf{x}_n)+\boldsymbol{\delta}_n\approx\mathbf{T}(\mathbf{x}_n)$. Under these circumstances, the embedding is always stable, and there is no detachment. In this regime we can compute explicitly the above-given expression, Eq. (22), which depends only on the current value of the position:

$$\tau(\mathbf{x})=\frac{\langle\boldsymbol{\delta}^2\rangle}{\langle\boldsymbol{\xi}^2\rangle}=\sum_{j=0}^{\infty}\left(e^{-j\gamma}\prod_{k=0}^{j}\boldsymbol{\nabla}\mathbf{T}|_{\mathbf{T}^{-k}(\mathbf{x})}\right)^2. \tag{23}$$

Thus $\tau(\mathbf{x})$ defines a sort of temperature for the fluctuations $\boldsymbol{\delta}$.

As long as the $\boldsymbol{\delta}$ are infinitesimally small, they do not—and cannot—affect the $\mathbf{x}$ dynamics, which has collapsed onto the classical trajectories; thus they do not influence the invariant density $P(\mathbf{x})$ either, and hence $P(\mathbf{x})$ is asymptotic to the Lebesgue measure. For infinitesimally small $\langle\boldsymbol{\xi}^2\rangle$, as γ is made smaller, the sum acquires more and more terms because the prefactor $e^{-j\gamma}$ decays more and more slowly. For any value of γ, the products of the gradients grow or shrink roughly as the exponential of the Lyapunov exponent times j. Thus, when γ equals the local Lyapunov exponent at $\mathbf{x}$, the series defining $\tau(\mathbf{x})$ stops being absolutely convergent at $\mathbf{x}$ and may blow up. As γ is lowered further, more and more points $\mathbf{x}$ have local Lyapunov exponents greater than γ, and so $\tau(\mathbf{x})$ formally diverges at more and more points $\mathbf{x}$.

Where $\tau(\mathbf{x})=\infty$ it means that $\langle\boldsymbol{\delta}_n^2\rangle$ is finite even if $\langle\boldsymbol{\xi}^2\rangle$ is infinitesimally small. Thus the embedding trajectories have detached from the actual trajectories, and the above-given approximations break down. Detachment is the process that we first envisioned as being characteristic of bailout embeddings.[16] However, by employing noise in the embedding, and carefully controlling its use, we can see the process that occurs before detachment. If $\tau(\mathbf{x})$ is finite and smaller than $1/\langle\boldsymbol{\xi}^2\rangle$, then we have a regime in which the $\boldsymbol{\delta}$'s behave as a noise term added to the classical trajectories: $\mathbf{x}_{n+1}=\mathbf{T}(\mathbf{x}_n)+\boldsymbol{\delta}_n$ with $\langle\boldsymbol{\delta}_n^2\rangle=\langle\boldsymbol{\xi}^2\rangle\tau(\mathbf{x})$.

We have lost the whiteness of the noise process, since $\boldsymbol{\delta}_{n+1}$ and $\boldsymbol{\delta}_n$ are not any longer statistically independent. However, this is secondary to the fact that the noise process amplitude, being modulated as a function of position, will immediately lead to inhomogeneity in the dynamics: hot regions will be avoided while cold regions will preserve the dynamics. All of this is in a context in which the embedding is essentially stable throughout. Thus this process is not detachment *per se*, but rather avoidance.

We can illustrate this best in the context of the standard map acting as before as the base flow. Figure 3 shows side by side the visit histogram—the invariant measure—(left-hand side) together with the corresponding space-dependent temperature (right-hand side) for a decreasing sequence of the bailout parameter γ and fixed values of the standard-map nonlinearity and noise parameters. While, for γ larger than 0.55, the temperature is a well-defined function of the space coordinates, it shows signs of divergence—the red regions, which become larger as γ decreases—for γ smaller than 0.55. On the other hand, however, the invariant measure displays features related to the structure of τ on both sides of this transition, i.e., even before detachment occurs.

VI. DISCUSSION AND CONCLUSIONS

It has previously been demonstrated that small neutrally buoyant particles immersed in a fluid flow, and therefore subject to drag forces, may follow trajectories that spontaneously separate from those of the fluid parcels in some regions of the flow. Specifically, this occurs when the strain is very

strong compared to the Stokes number of the particles. Given that, in general, the smaller the particles, the greater the strain necessary for this phenomenon to manifest itself, the conditions for separation to occur may not be fulfilled in some fluid flows of physical interest. However, we have shown here that the addition of noise to the forces acting on the particles can extend the action of this phenomenon beyond the range of Stokes numbers for which separation is possible in a deterministic system, allowing the generation of inhomogeneities in the asymptotic distributions of these particles even in cases where the flow is a highly efficient mixer.

There is a large variety of examples in which noise ought naturally to be added to the dynamical equations of particulate impurities. Thermal or concentration fluctuations, for instance, should be considered in a range of small-scale laboratory experiments. The effect of small-scale turbulence on drifters in oceanographic applications might be another relevant example. In the case of plankton dynamics, in which the emergence of inhomogeneous distributions is an issue, the autonomous swimming abilities of individuals might be viewed as an internal source of noise. But could the phenomenon described here be the basis of the plankton distribution patchiness? If each individual plankton is naively considered as an impurity particle, the answer is obviously no: their size is far too small for these effects to be appreciable. But if there are grounds to consider plankton in large-scale colonies moving more or less rigidly in the ocean, the consequences of the phenomenon described here need to be taken seriously.

We conclude with an epistemological note: the dynamics of neutrally buoyant particles in flows has suggested to us a generalization to maps that helps to solve some problems in the domain of Hamiltonian dynamics. This generalization in turn pays us back by suggesting a way in which inhomogeneous distributions may arise in fluid-dynamical problems. We believe that this is a remarkable instance of mutual support in the interdisciplinary marriage between the two fields.

ACKNOWLEDGMENTS

We should like to thank Leo Kadanoff, Rubén Pasmanter, and Marcelo Viana for useful discussions. J.H.E.C. acknowledges the financial support of the Spanish CSIC, Plan Nacional del Espacio Contract No. ESP98-1347. M.O.M. acknowledges the support of the Meyer Foundation. O.P. acknowledges the Spanish Ministerio de Ciencia y Tecnologia, Proyecto CONOCE, Contract No. BFM2000-1108.

[1] E. R. Abraham, Nature (London) **391**, 577 (1998).
[2] S. A. Levin and L. A. Segal, Nature (London) **259**, 659 (1976).
[3] *Spatial Patterns in Plankton Communities*, edited by H. J. Steele (Plenum, New York, 1978).
[4] C. Jung, T. Tél, and E. Ziemniak, Chaos **3**, 555 (1993).
[5] Z. Toroczkai *et al.*, Phys. Rev. Lett. **80**, 500 (1998).
[6] Z. Neufeld, C. López, and P. H. Haynes, Phys. Rev. Lett. **82**, 2606 (1999).
[7] A. Babiano, J. H. E. Cartwright, O. Piro, and A. Provenzale, in *Coherent Structures in Complex Systems*, Lecture Notes in Physics, Vol. 567, edited by D. Reguera, L. Bonilla, and M. Rubi (Springer, New York, 2001), pp. 114–126.
[8] A. Babiano, J. H. E. Cartwright, O. Piro, and A. Provenzale, Phys. Rev. Lett. **84**, 5764 (2000).
[9] M. Feingold, L. P. Kadanoff, and O. Piro, J. Stat. Phys. **50**, 529 (1988).
[10] O. Piro and M. Feingold, Phys. Rev. Lett. **61**, 1799 (1988).
[11] J. H. E. Cartwright, M. Feingold, and O. Piro, Physica D **76**, 22 (1994).
[12] J. H. E. Cartwright, M. Feingold, and O. Piro, J. Fluid Mech. **316**, 259 (1996).
[13] J. H. E. Cartwright, M. Feingold, and O. Piro, Phys. Rev. Lett. **75**, 3669 (1995).
[14] M. Abel, A. Celani, D. Vergni, and A. Vulpiani, Phys. Rev. E **64**, 046307 (2001).
[15] C. López *et al.*, Chaos **11**, 397 (2001).
[16] J. H. E. Cartwright, M. O. Magnasco, and O. Piro, Phys. Rev. E **65,** 045203(R) (2002).
[17] M. R. Maxey and J. J. Riley, Phys. Fluids **26**, 883 (1983).
[18] E. E. Michaelides, J. Fluids Eng. **119**, 233 (1997).
[19] G. I. Taylor, Proc. R. Soc. London, Ser. A **120**, 260 (1928).
[20] T. R. Auton, J. C. R. Hunt, and M. Prud'homme, J. Fluid Mech. **197**, 241 (1988).
[21] J. Boussinesq, C. R. Acad. Sci. Paris **100**, 935 (1885).
[22] A. B. Basset, Philos. Trans. R. Soc. London **179**, 43 (1888).
[23] H. Faxén, Ann. Phys. (Paris) **4**, 89 (1922).
[24] A. Okubo, Deep-Sea Res. **17**, 445 (1970).
[25] J. B. Weiss, Physica D **48**, 273 (1991).
[26] M. Büttiker, Z. Phys. B: Condens. Matter **68**, 161 (1987).
[27] R. Landauer, J. Stat. Phys. **53**, 233 (1988).